

Low dispersion broadband integrated double-slot microring resonators optical buffer

Chuan WANG, Xiaoying LIU (✉), Minming ZHANG, Peng ZHOU

School of Optical and Electronic Information, Huazhong University of Science and Technology, Wuhan 430074, China

© Higher Education Press and Springer-Verlag Berlin Heidelberg 2016

Abstract Microring resonator optical buffer is attractive in high-speed optical network system, but ordinary microring resonator use strip waveguide as its basic light guide medium, which cannot provide small footprint, low dispersion and high delay-bandwidth product (DBP) simultaneously. Double-slot waveguide structure was first proposed to construct racetrack-microring resonators. It was found that cascading multiple microrings can increase the delay-bandwidth and lower the dispersion of the resonators by optimizing the structure parameters. Optical buffer cascaded by 8 microrings with flat bandwidth of 20 GHz provided the delay of 150 ps and the dispersion of $\sim 10^{-7}$ ps/nm over 1530–1630 nm, and the footprint of each microring was about $51\mu\text{m}^2$. This study can provide design methods and theoretical basis support for practical application.

Keywords optical buffer, microring, resonator, delay, slot, waveguide, dispersion

1 Introduction

As a key part of all optical communication, all optical switch has become a hot topic with the development of all optical communication over the years. All optical buffer is one of the core components of all optical switch network which solves the problem of competition of burst communications, a common occurrence in high speed optical network. At present, the most studied types of all optical buffer can be classified into electromagnetically induced transparency (EIT) based slow light effect, fiber delay line structure, photonic crystal structure and optics microring resonator structure [1–4]. The EIT slow light buffer has high costs and complicated system structure and

manufacturing process, therefore it is hard to apply. Optical buffer made of fiber delay lines has large size, and it cannot be easily integrated into microsystems. The optical microring resonators are small-size and high integrated optical device, optical buffers with photonic crystal structure have comparable characteristics but they have demonstrated to have inferior optical performance, tunability, flexibility and reproducibility. Besides optical buffers, the microring resonator structure can be used to construct filters, wavelength transformers, modulators, optical transmitters, and optical switches [5]. They can be built on-chip and have the best tunability and flexibility [6,7]. The main challenges in recent researches on optical microring resonator buffers, are the limited delay-bandwidth of single-ring resonator optical buffers and the impossibility of decreasing the size and dispersion of multi-ring resonator optical buffers simultaneously [6]. Our aim in this study is to design a kind of all optical buffer which has the properties of small size, big delay and low dispersion.

Slot waveguide is a new kind of waveguide structure, in the middle of which there are one or more slots made from low index materials [8]. The slot waveguides have increased waveguide confinement of light and dispersion sensitivity to the structure [9–11], and show the properties of tailorable broadband and low dispersion [12–15]. Among various slot waveguide structures, the double-slot waveguide reaches the best compromise between the performance and manufacturing feasibility of these structures [16,17]. The reason we choose the waveguide with two slots as the basic structure is that more slots means too complicated structures to design and manufacture, while double-slot is enough to provide light confinement, flexibility and tailorability of optical properties (for example, dispersion).

In fabrication, the size of microring has been reduced gradually, radius as low as $1\mu\text{m}$ while the insertion loss is 1 dB [18]. Microring can be fabricated using an electron-beam-lithography (EBL)-based fabrication process or fully

complementary metal oxide semiconductor (CMOS) compatible processes, such as deep ultraviolet lithography. The non-uniformity in the fabrication process of the device will result in some unwanted performance, such as the variations of the coupling coefficient and the resonance wavelength of single ring, and the problem of mismatch between multiple rings [7]. To solve these problems, researchers made use of advanced patterning and process design, such as the CMOS pilot line at IMEC (Leuven, Belgium), the 193 nm optical lithography (ASML/1100) and dry etching [19], the device uniformity less than 1% with low loss was achievable [20–23]. Accurate post-fabrication trimming (PFT) technology could be used to stabilize the device performance [24].

In this paper, we use dispersion optimized slot waveguides to construct the microring resonators, basing on the Vernier effect [25], and then optimize the device parameters to realize an optical buffer with low-dispersion, broadband and flat-high-delay.

2 Theoretical methods

2.1 Structure of double slot microring resonator optical buffer

Racetrack microring resonators, shown in Figs. 1(a) and 1(b), were made of double-slot waveguide (see Fig. 1(c)). We used silicon with high index as waveguide material, and silica with low index was adopted as slot and substrate material (the thickness of substrate is 2 μm). These resonators composed of one racetrack microring waveguide and one straight waveguide. Both waveguides had

double-slot structure. The length of the straight part in the racetrack microring is l_c while the radius of the semicircular part is R (Fig. 1(a)). The coupling area between two straight waveguides is shown in the dashed box in Fig. 1(a). The coupling gap g is defined as the gap between two straight waveguides and the coupling length equals the length of straight part, l_c .

The loss of the microring in Fig. 1(a) consists of three parts: the loss of the straight part L_{straight} , the loss of the semicircular track part $L_{\text{full-ring}}$, and the mismatch loss caused by mode coupling between two waveguides L_{mismatch} .

The structure of multi-ring resonator optical buffer is shown in Fig. 2. Cascading multi-ring will increase the total delay [25,26], and the total spectrum equals the sum of those single-ring delay spectrums [27]. When each ring in the multi-ring resonator optical buffer has different parameters, they will have different resonance wavelengths, and the total delay spectrum bandwidth will increase, according to the Vernier effect. Using appropriate parameters can make the total bandwidth increase with the number of rings.

2.2 Dispersion tailorability of the double-slot waveguide

The main guided mode in double-slot waveguide changes with transmission wavelength. As the wavelength becomes longer, a quasi-strip mode in the middle-layer silicon at short wavelength will transfer into a quasi-slot mode in the slot [12,28,29]. The dispersion characteristic varies dramatically with the wavelength. As the guided mode depends largely on the waveguide structure, we can do fine adjustment on the total dispersion by adjusting the

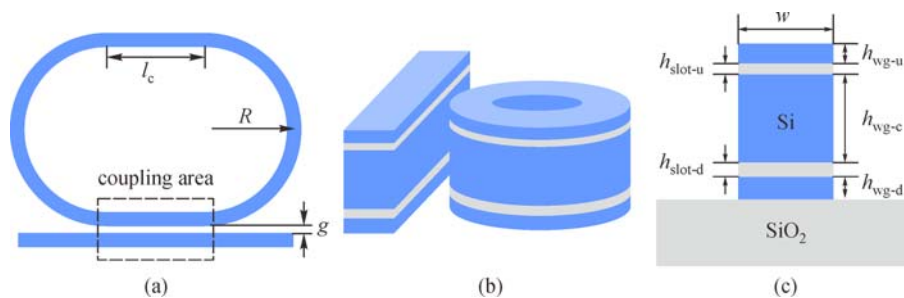


Fig. 1 (a) Basic structure and (b) perspective view of racetrack microring resonator; (c) structure of double-slot waveguide made of racetrack microring resonator

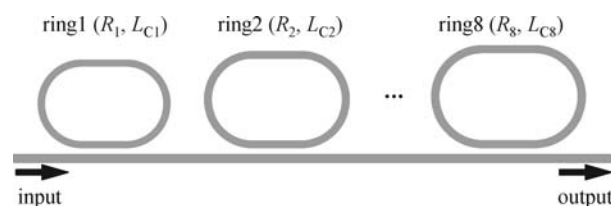


Fig. 2 Structure of multiple microrings optical buffer

structural parameters accurately [28,30–32].

The optimum dispersion characteristic of one straight waveguide structure can be obtained through structural optimization. While when the waveguide turns into bending state, there will be degradation, since the dispersion is effected by the shape of the waveguide [13], and the more it bends the more the dispersion characteristic degrades. We figured out two possible solutions to get desired dispersion characteristic. The first solution is to deploy bigger radius of the semicircular waveguide and avoid obvious dispersion deterioration. The other solution is to use different waveguide structure in the straight and the semicircular part, and optimize them respectively and try to make the total dispersion as low as possible. To reduce the device size to the greatest extent, the second solution is chosen. When we use different waveguide structure for straight and bend waveguides, another matter needs to be considered is that the guided mode distributions are different in different waveguides, so there will be mismatch loss at the junctions. Smaller mismatch losses are expected.

Through simulation, the dispersion characteristic of straight double-slot waveguide with $w = 600$ nm, $h_{\text{wg-u}} = 100$ nm, $h_{\text{wg-c}} = 384$ nm, $h_{\text{wg-d}} = 112$ nm, $h_{\text{slot-u}} = 42$ nm, $h_{\text{slot-d}} = 72$ nm are obtained, as given by the solid line in Fig. 3, and it shows flatness in communication wavelengths (1.53–1.63 μm). The dispersion value is $-14-0.5$ ps/(nm \cdot km) and the flatness (ratio of dispersion range and bandwidth) is 0.135 ps/(nm 2 \cdot km). After switching to the 3 μm radius bending state, the optimized waveguide structural parameters are changed to $h_{\text{wg-d}} = 82$ nm, $h_{\text{slot-u}} = 60$ nm, $h_{\text{slot-d}} = 102$ nm (other parameters are unchanged). The dispersion value is $-14-2.9$ ps/(nm \cdot km) and the flatness is 0.169 ps/(nm 2 \cdot km), as shown by the dash line in Fig. 3.

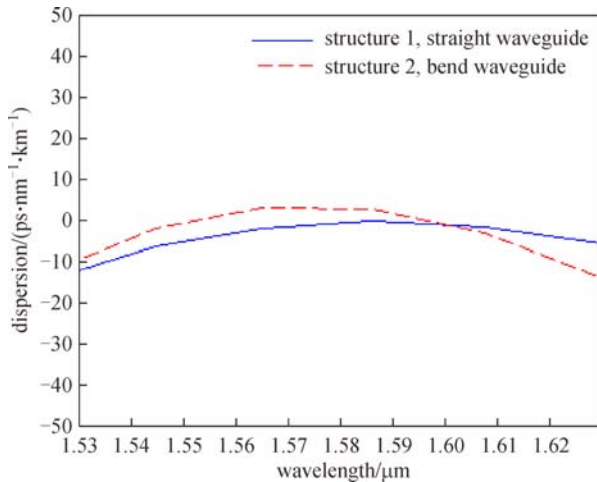


Fig. 3 Dispersion spectrum of optimized straight and bent double-slot waveguide

2.3 Transmission performance of microring resonators optical buffer

We analyzed the microring according to the optical waveguide coupled-mode theory and the transfer matrix method. The normalization delay of a microring is [33,34]:

$$T_{\text{delay}} = 1 + \frac{t\alpha\cos\phi - t^2}{\alpha^2 + t^2 - 2\alpha t\cos\phi} + \frac{\alpha t\cos\phi - \alpha t^2}{1 - 2\alpha t\cos\phi + \alpha^2 t^2},$$

where t is the self-coupling coefficient, representing the couple efficient between the microring waveguide and the straight waveguide. α is the round-trip propagation loss, representing the loss of the microring waveguide. $\phi = \beta l$ is the effective phase shift, where l is the microring perimeter. $\beta = 2\pi n_{\text{eff}}/\lambda$, where n_{eff} is the effective refractive index of the microring waveguide.

The microring delay performance is related to the microring perimeter, the self-coupling coefficient and the round-trip propagation loss factor. The microring perimeter affects the resonance wavelength and the maximum delay time. The self-coupling coefficient and the round-trip propagation loss affect the Q -factor and the fineness of the delay spectrum, we need to adjust the dimension of the coupling area of the microring resonator, so the coupling efficient can be tailored.

2.4 Structure design

The structural design contains three parts. First is to analyze the loss factor of the racetrack microring waveguide and deduce a formula to calculate the round-trip propagation loss according to structural parameters. The second part is about the coupling coefficient in the coupling area, between the racetrack microring waveguide and the straight waveguide. We need a relation of the self-coupling coefficient and structural parameters. After the first two parts, we will have two formulas, representing the relation of loss factor and the coupling coefficient to the device structure parameters. The last part is to import the formulas into a MATLAB program and calculate the multi-ring resonator's total delay spectrum, and then adjust the input parameters to get an optimum flattened delay performance.

3 Simulation results

3.1 Loss simulation of racetrack microring waveguide

All simulations were based on finite different time domain (FDTD) method. When the double-slot waveguide is unbend, the loss per unit length is $a = 30.7$ dB/cm at wavelength 1.55 μm . l_c is the length of the straight part in the microring waveguide which consists a upper one and a

lower one, so the straight waveguide loss L_{straight} is proportional to l_c (where the length unit of l_c is micrometer).

$$L_{\text{straight}} = 2l_c a = 0.0061l_c.$$

Similarly, the loss per unit length of bend double-slot waveguide of radius R is a_{bend} . A racetrack microring contains left and right semicircular track, so the bend waveguide loss $L_{\text{full-ring}}$ is

$$L_{\text{full-ring}} = 2\pi R a_{\text{bend}}.$$

We simulated the changing curve of a_{bend} and $L_{\text{full-ring}}$ with R from 1.5 to 11 μm , as shown in Fig. 4. Its fitting formula is shown by the dotted line in Fig. 4, the unit of R is micrometer:

$$L_{\text{full-ring}} = 0.0197R + 0.0016.$$

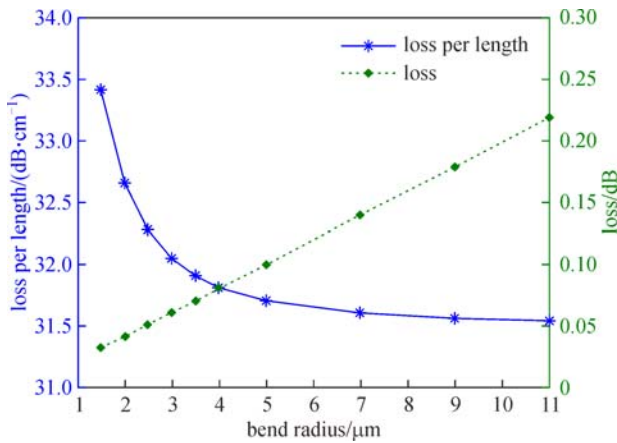


Fig. 4 Bend loss of microring with various ring radiuses

In one microring, there are 4 joint of straight and semicircular waveguides, and therewith 4 mode mismatching. The overlap ratio p of modes in straight track and semicircular track was simulated. The mode mismatch loss L_{mismatch} calculates as

$$L_{\text{mismatch}} = 4(-10\log p).$$

The simulation result of the relation between L_{mismatch} and R are shown in Fig. 5. The fitting formula is shown by the dotted line in Fig. 5, the unit of R is micrometer:

$$L_{\text{mismatch}} = 0.6466R^{-1.705}.$$

To sum up the above, the total loss L can be represented as

$$\begin{aligned} L &= L_{\text{straight}} + L_{\text{full-ring}} + L_{\text{mismatch}} \\ &= 0.0061l_c + 0.0197R + 0.0016 + 0.6466R^{-1.705}. \end{aligned}$$

So the round-trip propagation loss α is

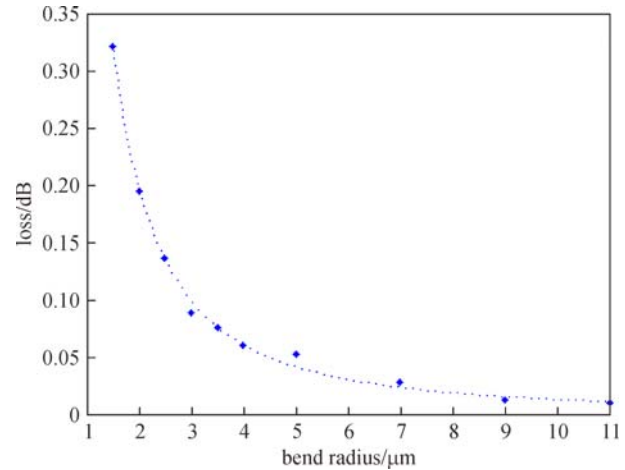


Fig. 5 Mismatch loss with various ring radiuses

$$\alpha = 10^{-\frac{L}{10}} = 10^{-[(0.0061l_c + 0.0197R + 0.0016 + 0.6466R^{-1.705})/10]}.$$

3.2 Simulation results of the coupling area in microrings

As shown in Fig. 1, in the coupling area, two straight waveguides have a gap of g . The gap determines the difficulty of mode coupling. When the waveguide structure is fixed, the length and width of the resonator coupling area decide together the value of the self-coupling coefficient. Using FDTD method, we can get the mode effective refractive index difference Δn of light transmitting in the coupling area, and then calculate the relation of the coupling coefficient of microring resonant and the coupling area length.

Assume that the initial power in waveguide 1 is P_0 . After transmitting for a distance l_t , the power in waveguide 2 is

$$P_2(l_t) = P_0 \sin^2\left(\frac{\pi l_t \Delta n}{\lambda}\right).$$

The power coupling coefficient can be defined as the ratio of power coupled from waveguide 1 to waveguide 2 and it has a relation with l_t :

$$\tau = \frac{P_2(l_t)}{P_0} = \sin^2\left(\frac{\pi l_t \Delta n}{\lambda}\right).$$

We simulated waveguides with coupling gap 10–110 nm and calculated the corresponding full-coupling length (the transmission length it needs for light to couple from one waveguide to the other waveguide) and effective refractive index difference, as depicted in Fig. 6. When the gap becomes larger, it is more difficult for light to couple, so the full-coupling length will increase correspondingly.

When design the microring resonators, we need to choose an appropriate coupling gap. If it is too wide, the coupling length will increase and make the device large. When the gap is too narrow, it is hard to realize in

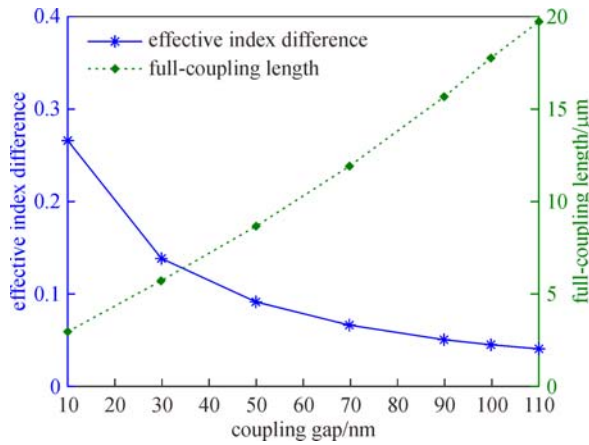


Fig. 6 Full-coupling length and index difference with various coupling gap

engineering. When taking the coupling gap as 10 nm, the corresponding effective refractive index difference Δn is 0.2653 and the full-coupling length is 2.921 μm .

3.3 Structure design and optimization of multi-ring optical buffer

We constructed an optical buffer of bandwidth 20 GHz with 8 microrings, the central wavelength is 1.55 μm . Basing on MATLAB program and the fitting formula of the round-trip propagation loss factor α and the coupling coefficient of microrings, we adjusted the structural parameters of 8 microring resonators, and calculated the total delay spectrum. Finally, we got the optimum parameters which make the spectrum top-flattened.

Figure 7 is the total delay spectrum of 3 different optimization results, the result 1 has the least optimization degree and result 3 has the most optimization degree. With greater optimization degree, the total delay spectrum has

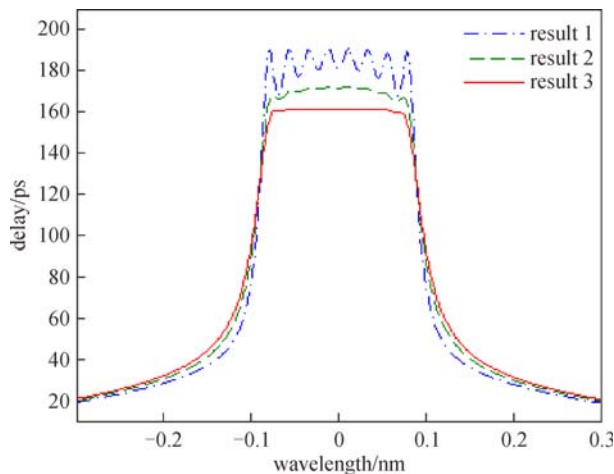


Fig. 7 Optimization results of total delay spectrum

flatter top and higher average delay. The average delay for results 1–3 are 170, 160 and 150 ps.

The result 3 in Fig. 7 is the final result. The corresponding structural parameters are shown in Table 1. The single-ring loss L is 0.164–0.189 dB, the round-trip propagation loss factor α is 0.957–0.963, the footprint is about 41–61 μm^2 .

Table 1 Structure parameters, loss and dispersion for 8 microrings

ring index	t	$l_c/\mu\text{m}$	$R/\mu\text{m}$	L/dB	α	$D/(\text{ps}\cdot\text{nm}^{-1})$
1	0.9547	2.360	2.673	0.189	0.957	-1.56×10^{-6}
2	0.9538	2.354	2.773	0.184	0.958	-1.08×10^{-6}
3	0.9531	2.350	2.872	0.179	0.959	-6.13×10^{-7}
4	0.9528	2.348	2.970	0.175	0.960	-1.47×10^{-7}
5	0.9527	2.347	3.069	0.172	0.961	3.11×10^{-7}
6	0.9529	2.348	3.166	0.169	0.962	7.56×10^{-7}
7	0.9533	2.351	3.263	0.166	0.962	1.19×10^{-6}
8	0.9543	2.356	3.359	0.164	0.963	1.60×10^{-6}

4 Discussion

According to the waveguide dispersion simulation results and the structural parameters of 8 microrings in Table 1, the dispersion of the microring resonator optical buffer can be calculated: at wavelength 1.55 μm , the straight waveguide dispersion is -2×10^{-8} ps/nm, the bend waveguide dispersion range is -1.5×10^{-6} – 1.6×10^{-6} ps/nm. So the straight dispersion can be ignored and the dispersion of microring resonator mainly comes from the bend part. Table 1 also shows the dispersions of 8 rings. The dispersions increase from negative to positive, therefore they can be partly compensated by each other. The total dispersion is 4.48×10^{-7} ps/nm.

5 Conclusions

The simulation results in this paper showed that the optical buffer has small size, low dispersion and flat and high delay in broadband wavelength. We constructed the optical buffer of 1.55 μm central wavelength, 150 ps delay in 20 GHz bandwidth with 8 microrings, and the total dispersion is $\sim 10^{-7}$ ps/nm. The average device size is only 51 μm^2 , which offers the advantage for integration. By adding more microrings, optical buffer with higher delay and broader bandwidth can be easily realized, which can be used in high speed optical communication system.

Acknowledgements This work was supported by the National Natural Science Foundation of China (Grant No. 61107051) and National High-tech R&D Program (No. SS2012AA010407).

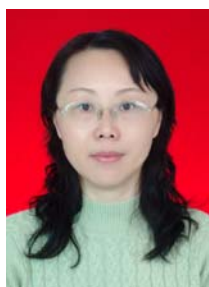
References

1. Melloni A, Morichetti F. The long march of slow photonics. *Nature Photonics*, 2009, 3(3): 119–119
2. Sheng X, Dong X, Zhang X, Peng C. Advances in the research on all-optical buffers. *Study on Optical Communications*, 2012, (6): 52–55
3. Dutta M K, Chaubey V K. Modeling and performance analysis of optical packet switching network using fiber delay lines. In: *Proceedings of India Conference*. 2011, 1–4
4. Melloni A, Canciamilla A, Ferrari C, Morichetti F, O'Faolain L, Krauss T, De La Rue R, Samarelli A, Sorel M. Tunable delay lines in silicon photonics: coupled resonators and photonic crystals, a comparison. *IEEE Photonics Journal*, 2010, 2(2): 181–194
5. Xia F, Sekaric L, Vlasov Y. Ultracompact optical buffers on a silicon chip. *Nature Photonics*, 2007, 1(1): 65–71
6. Morichetti F, Ferrari C, Canciamilla A, Melloni A. The first decade of coupled resonator optical waveguides: bringing slow light to applications. *Laser & Photonics Reviews*, 2012, 6(1): 74–96
7. Bogaerts W, De Heyn P, Van Vaerenbergh T, De Vos K, Selvaraja S K, Claes T, Dumon P, Bienstman P, Van Thourhout D, Baets R. Silicon microring resonators. *Laser & Photonics Reviews*, 2012, 6(1): 47–73
8. Almeida V R, Xu Q, Barrios C A, Lipson M. Guiding and confining light in void nanostructure. *Optics Letters*, 2004, 29(11): 1209–1211
9. Jágorská J, Thomas N L, Houdré R, Bolten J, Moormann C, Wahlbrink T, Ctyroky J, Waldow M, Först M. Dispersion properties of silicon nanophotonic waveguides investigated with Fourier optics. *Optics Letters*, 2007, 32(18): 2723–2725
10. Di Falco A, O'Faolain L, Krauss T F. Dispersion control and slow light in slotted photonic crystal waveguides. *Applied Physics Letters*, 2008, 92(8): 083501
11. Zheng Z, Iqbal M, Liu J. Dispersion characteristics of SOI-based slot optical waveguides. *Optics Communications*, 2008, 281(20): 5151–5155
12. Willner A E, Zhang L, Yue Y. Tailoring of dispersion and nonlinear properties of integrated silicon waveguides for signal processing applications. *Semiconductor Science and Technology*, 2011, 26(1): 014044
13. Zhang L, Yue Y, Beausoleil R G, Willner A E. Analysis and engineering of chromatic dispersion in silicon waveguide bends and ring resonators. *Optics Express*, 2011, 19(9): 8102–8107
14. Bao C, Yan Y, Zhang L, Yue Y, Willner A E. Tailoring of low chromatic dispersion over a broadband in silicon waveguides using a double-slot design. In: *Proceedings of Conference on Laser and Electro-Optics*. 2013, JTU4A.53-1–JTU4A.53-2
15. Yan Y, Matsko A, Bao C, Maleki L, Willner A E. Increasing the spectral bandwidth of optical frequency comb generation in a microring resonator using dispersion tailoring slotted waveguide. In: *Proceedings of IEEE Photonics Conference*. 2013, 230–231
16. Bao C, Yan Y, Zhang L, Yue Y, Ahmed N, Agarwal A M, Kimerling L C, Michel J, Willner A E. Increased bandwidth with flattened and low dispersion in a horizontal double-slot silicon waveguide. *Journal of the Optical Society of America B, Optical Physics*, 2015, 32(1): 26–30
17. Sun R, Dong P, Feng N N, Hong C Y, Michel J, Lipson M, Kimerling L. Horizontal single and multiple slot waveguides: optical transmission at $\lambda = 1550$ nm. *Optics Express*, 2007, 15(26): 17967–17972 PMID:19551093
18. Prabhu A M, Tsay A, Han Z, Van V. Extreme miniaturization of silicon add-drop microring filters for VLSI photonics applications. *IEEE Photonics Journal*, 2010, 2(3): 436–444
19. Selvaraja S K, Jaenen P, Bogaerts W, Van Thourhout D, Dumon P, Baets R. Fabrication of photonic wire and crystal circuits in silicon-on-insulator using 193-nm optical lithography. *Journal of Lightwave Technology*, 2009, 27(18): 4076–4083
20. Selvaraja S K, Bogaerts W, Dumon P, Van Thourhout D, Baets R. Subnanometer linewidth uniformity in silicon nanophotonic waveguide devices using CMOS fabrication technology. *IEEE Journal of Selected Topics in Quantum Electronics*, 2010, 16(1): 316–324
21. Selvaraja S K, De Vos K, Bogaerts W, Bienstman P, Van Thourhout D, Baets R. Effect of device density on the uniformity of silicon nano-photonic waveguide devices. In: *Proceedings of IEEE LEOS Annual Meeting Conference*. 2009, 311–312
22. Xiao S, Khan M H, Shen H, Qi M. Compact silicon microring resonators with ultra-low propagation loss in the C band. *Optics Express*, 2007, 15(22): 14467–14475
23. Bogaerts W, Selvaraja S K, Dumon P, Brouckaert J, De Vos K, Van Thourhout D, Baets R. Silicon-on-insulator spectral filters fabricated with CMOS technology. *IEEE Journal of Selected Topics in Quantum Electronics*, 2010, 16(1): 33–44
24. Atabaki A H, Askari M, Eftekhari A A, Adibi A. Accurate post-fabrication trimming of silicon resonators. In: *Proceedings of IEEE International Conference on Group IV Photonics GFP*. 2012, 42–44
25. Boeck R, Chrostowski L, Jaeger N A. Thermally tunable quadruple Vernier racetrack resonators. *Optics Letters*, 2013, 38(14): 2440–2442
26. Shinobu F, Ishikura N, Arita Y, Tamanuki T, Baba T. Continuously tunable slow-light device consisting of heater-controlled silicon microring array. *Optics Express*, 2011, 19(14): 13557–13564
27. Fontaine N K, Yang J, Pan Z, Chu S, Chen W, Little B E, Ben Yoo S J. Continuously tunable optical buffering at 40 Gb/s for optical packet switching networks. *Journal of Lightwave Technology*, 2008, 26(23): 3776–3783
28. Zhu M, Liu H, Li X, Huang N, Sun Q, Wen J, Wang Z. Ultrabroadband flat dispersion tailoring of dual-slot silicon waveguides. *Optics Express*, 2012, 20(14): 15899–15907
29. Subbaraman H, Ling T, Jiang Y, Chen M Y, Cao P, Chen R T. Design of a broadband highly dispersive pure silica photonic crystal fiber. *Applied Optics*, 2007, 46(16): 3263–3268
30. Yoo H G, Fu Y, Riley D, Shin J H, Fauchet P M. Birefringence and optical power confinement in horizontal multi-slot waveguides made of Si and SiO₂. *Optics Express*, 2008, 16(12): 8623–8628
31. Yang S H, Cooper M L, Bandaru P R, Mookherjea S. Giant birefringence in multi-slotted silicon nanophotonic waveguides. *Optics Express*, 2008, 16(11): 8306–8316
32. Ding R, Baehr-Jones T, Kim W, Boyko B, Bojko R, Spott A, Pomerene A, Hill C, Reinhardt W, Hochberg M. Low-loss asymmetric strip-loaded slot waveguides in silicon-on-insulator. *Applied Physics Letters*, 2011, 98(23): 233303

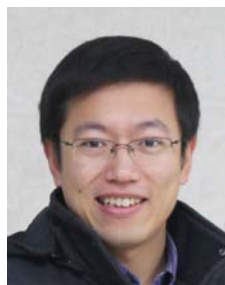
33. Uranus H P, Hoekstra H J W M. Modeling of loss-induced superluminal and negative group velocity in two-port ring-resonator circuits. *Journal of Lightwave Technology*, 2007, 25(9): 2376–2384
34. Lou F. Theoretical study on microring resonators based all optical buffers. Dissertation for the Doctoral Degree. Wuhan: Huazhong University of Science and Technology, 2011, 21–27



Chuan WANG received the M.S. degree from the School of Optical and Electronic Information, Huazhong University of Science and Technology, Wuhan, China, in 2015. Her field of research include simulation and designing of optical devices, such as optical buffers and system performance analyze of optical network.



Xiaoying Liu is an Associate Professor in the School of Optical and Electronic Information at Huazhong University of Science and Technology, Wuhan, China. She was a postdoctoral researcher of College of Optoelectronics Science and Technology at Huazhong University of Science and Technology in 2003. Her current research includes micro-ring resonators, advanced modulation formats, all-optical tunable filter, optical fiber sensor and wireless sensor network.



Minming Zhang received the B.S., M.S., and Ph.D. degrees in Electronic Science and Technology from Huazhong University of Science and Technology (HUST), Wuhan, China, in 1998, 2001, and 2007 respectively. He is currently an Associate Professor of Optical Engineering at the School of Optical and Electronic Information of HUST. He has published more than 40 papers in journals and conference proceedings. His research interest has centered on the advanced silicon photonic devices and all optical signal processing.



Peng Zhou received the B.S. degree from the School of Optical and Electronic Information, Huazhong University of Science & Technology. He is currently working toward the Ph.D. degree in Electrical and Computer Engineering department, University of Maryland, United State of America. His research includes optical communication system, optical devices and Nano photonics.